

EXPERIMENTAL DETERMINATION OF THE TRANSIENT TRANSPORT AND OF FLUCTUATIONS RELEVANT TO TRANSPORT IN ASDEX

H. NIEDERMEYER, G. DODEL¹, M. ENDLER, G. FUSSMANN,
O. GEHRE, K.W. GENTILE², L. GIANNONE, E. HOLZHAUER¹,
K. KRIEGER, A. RUDYJ, G. THEIMER, R.D. BENGTSON²,
A. CARLSON, A. EBERHAGEN, W. ENGELHARDT, J. GERNHARDT,
O. GRUBER, J.V. HOFMANN, F. KARGER, O. KLÜBER,
M. KRÄMER³, M.E. MANSO⁴, J. MATIAS⁴,
K. McCORMICK, V. MERTENS, H.D. MURMANN, J. NEUHAUSER,
J. QIN⁵, N. RUHS, F. RYTER, U. SCHNEIDER, R. SCHUBERT,
F. SERRA⁴, A. SILVA⁴, F.X. SÖLDNER, U. STROTH,
N. TSOIS⁶, O. VOLLMER
Max-Planck-Institut für Plasmaphysik,
Euratom-IPP Association,
Garching, Federal Republic of Germany

Abstract

EXPERIMENTAL DETERMINATION OF THE TRANSIENT TRANSPORT AND OF FLUCTUATIONS RELEVANT TO TRANSPORT IN ASDEX.

Particle transport was studied in ASDEX with modulated puffing of the discharge gas and of impurities. The energy transport is investigated by numerical simulation of the heat pulse after the sawtooth crash. Small scale density fluctuations are investigated in the confinement region with far infrared scattering and reflectometry and in the edge plasma with Langmuir probes and H_α diagnostic. In addition to a diffusive component of the particle transport, a strong inward drift is observed in all discharges. In ohmic discharges the transport coefficients decrease and saturate like $1/\tau_E$ with increasing density. They are smaller in deuterium than in hydrogen. In the improved ohmic confinement (IOC) regime mainly D in the outer region is reduced. D increases proportionally to the heating power in L-mode discharges. The improvement of particle confinement in the H-mode is explained by an increase of the inward drift at the edge rather than a decrease of D. The impurity diffusion coefficient is independent of the impurity mass and charge. In ohmic discharges, it varies with n_e like the bulk diffusion coefficient, is independent of B or increases weakly with B and increases with I_p . In L-mode discharges, D_{imp} increases linearly with the heating power. The electron thermal conductivity determined by heat pulse propagation exceeds the stationary value by a factor of 3-4, assuming merely diffusive heat transport. Convection does not significantly reduce this factor. However, non-diagonal terms

¹ Universität Stuttgart, Federal Republic of Germany.

² University of Texas, Austin, USA.

³ Ruhr-Universität Bochum, Federal Republic of Germany.

⁴ Instituto Superior Tecnico, Lisbon, Portugal.

⁵ Institute of Physics, Beijing, China.

⁶ National Research Centre for the Physical Sciences Democritos, Athens, Greece.

in a general transport equation system may remove the discrepancy. Drift-type turbulence with a remarkable radial asymmetry is found. The Doppler shift due to plasma rotation complicates the interpretation of frequency spectra. No separate ion feature could be identified. In the L-mode an increase of the fluctuation level together with a broadening of the frequency spectra and a shift of the k-spectra to small values are observed. During L-H transitions the fluctuation level drops immediately. However, during ELM free H-phases the fluctuation level can in some cases begin to grow again. The particle transport at the edge can be explained by the fluctuating $n \cdot E \times B$ flux derived from probe measurements. Like the core turbulence, these flute-like fluctuations show an inboard-outboard asymmetry. This suggests that bad curvature is a key element of the driving mechanism. Because of the high correlation of density fluctuations along the magnetic field lines, the interaction with the target plates may be important.

1 INTRODUCTION

The mechanism responsible for the anomalous transport of energy and particles generally observed in tokamaks is not yet well understood, even though this phenomenon is as exciting as it is important for the development of a fusion reactor. It is accepted by the majority of the fusion community that microscopic fluctuations are involved and that they lead not only to enhanced heat and particle diffusion coefficients but also to anomalous off-diagonal transport coefficients. This paper reports on work performed in order to obtain better insight both into spatial and parameter variations of the coefficients using transient particle and heat fluxes and into the nature of fluctuations suspected as driving the transport.

2 TRANSPORT IN THE BULK PLASMA

2.1 Method

Small density perturbations about equilibrium, induced by sinusoidal modulation of the gas valve, were analyzed for different radial channels of the ASDEX HCN-laser-interferometer. The measured amplitudes and phase shifts are compared to solutions of the particle conservation equation, $\partial n / \partial t = -\nabla \cdot \Gamma + P$. A transport law with a diffusive and a convective component $\Gamma = -D \nabla n - Vn$ is assumed. The coefficients $D(r)$ and $V(r)$ are determined with a crude radial resolution by a numerical fitting method [1].

2.2 General observations

Discharges with different heating methods, densities, plasma currents, toroidal fields and hydrogen isotopes have been investigated [2]. In all cases a strong inward particle drift V was observed. Transport coefficients are generally larger in the outer region of the plasma.

2.3 Ohmic discharges

A general decrease in transport coefficients both in the interior and the outer part of the plasma with increasing density is observed. However, the decrease saturates at higher density, an effect especially pronounced in the diffusion coefficients. Furthermore, there is a strong isotope effect, that is all coefficients but V in the outer region are much smaller for deuterium compared to hydrogen. Coefficients in the interior are significantly lower than those in the exterior at nearly every density.

The dependence of D and V on other parameters is more complex and less strong. There is a clear tendency for D in the center to increase with I_p , probably due to increased sawtooth activity. For the outer portion of the plasma, the only systematic effect is that D increases with toroidal field.

The most significant difference between the Improved Ohmic Confinement regime (IOC) and the saturated regime is a reduction of the outer D by a factor reaching 4 at the highest densities.

2.4 L-mode discharges

In co-injection heated discharges, D in the outer region increases proportional to the neutral injection power. The central value of D increases strongly at small power and has a general weak tendency to increase with further increasing power. The increase of D in the outer region with heating power is very large at low plasma current, but less pronounced with higher plasma currents. Diffusion in the core is largely unaffected. The current dependence of particle transport in L-mode is however mainly an effect of q , as shown by a magnetic field variation at constant I_p .

2.5 H-mode discharges

A steady-state H-mode with grassy ELMs was investigated. The value of D in the confinement zone during the H-mode remains at its elevated L-mode value. In contrast, the convective velocity in the periphery increases strongly, by a factor of 3-5. This explains the improved particle confinement and is consistent with the density pedestal observed.

3 TRANSPORT OF IMPURITIES

3.1 Method

A harmonic analysis method similar to the one discussed above for the background plasma was applied to impurity transport [3]. In this case trace impurities such as SiH_4 , H_2S , and HBr are puffed into the plasma with sinusoidal modulation in time using a programmed valve. Harmonic analysis of the measured line radiation in several spectral ranges from visible to X-ray

allows determination of phase relations and Fourier amplitudes at the modulation frequency.

3.2 Theory

The solution of the transport equation for each impurity is calculated assuming a sinusoidal time dependence and a simple model for the transport coefficients, with diffusion $D = \text{const.}$ and drift $V \sim r$. By comparing the calculated phase shifts and Fourier amplitudes at a given frequency with the corresponding measured values, it is possible to determine the transport parameters within the scope of the simplified model. Since the Fourier amplitudes of the total impurity density could not be measured, the analysis is restricted to the determination of the diffusion coefficient. This is possible from the measured phase alone due to its weak dependence on the drift velocity.

As a matter of basic interest, we note that the method of harmonic analysis offers also the possibility of determining both transport quantities D and V as functions of the radius, provided that the amplitude A and phase φ of the total impurity density have been accurately measured. Integration of the source free transport equation leads to the integral transforms

$$D(r) = -\frac{\omega}{r\varphi'(r)} \int_0^r dr' r' \frac{A(r')}{A(r)} \cos(\varphi(r') - \varphi(r))$$

$$V(r) = -\frac{\omega}{r} \int_0^r dr' r' \frac{A(r')}{A(r)} \sin(\varphi(r') - \varphi(r)) + \frac{A'(r) D(r)}{A(r)}$$

3.3 Parameter range

Diffusion coefficients, derived by means of the analysis described above, were determined for ohmic and NI-heated L-mode discharges with varying plasma parameters [3], [4].

3.4 Ohmic discharges

We observed that the diffusion coefficient is independent of the charge (and mass) of the ions as expected from the predictions of neoclassical theory. On the other hand, we find that the diffusion coefficient decreases with increasing electron density. Furthermore, at fixed density the diffusion coefficient seems to be constant or even increase slightly with the toroidal magnetic field. It also increases with the plasma current. These results are in complete contradiction to the neoclassical theory of impurity transport. Thus the results obtained can only be understood in terms of an additional

anomalous diffusion dominating the transport processes. This behavior is in striking contrast to the non-stationary accumulation phases found in discharges with improved energy and particle confinement [5].

3.5 L-mode discharges

For L-mode discharges the dependence of the diffusion coefficient on the NI heating power was investigated. The results show an approximately linear increase with the injected power.

As a final remark, we note that the diffusion coefficients presented agree well with results from earlier measurements using laser ablation and impurity doped pellets.

4 HEAT PULSE TRANSPORT

4.1 Method

The local electron temperature is measured at four radial positions outside the mixing radius by the ECE diagnostic and the signal is sampled at 20 kHz to provide sufficient time resolution of the sawtooth crash and the resultant heat pulse. In Ohmic discharges the sawtooth period is 5 -10 ms. Boxcar averaging of the temperature perturbation permits the electron thermal conductivity, χ_e , to be determined. The time dependent temperature perturbation at each radial position is fitted by the numerical solution of the heat pulse propagation equation as a forced boundary value problem [6]. The first channel outside the mixing radius is used as the time dependent boundary condition. In contrast to particle transport, there is no generally accepted ansatz for the heat transport equation.

4.2 Results

Assuming a transport law $Q = -n\chi\partial T/\partial r$ for electrons and ions, heat pulse values of χ_e are generally a factor of 3 higher than equilibrium values. In this approximation the density pulse associated with a sawtooth crash is neglected, because the relative amplitude of the density perturbation in these Ohmic discharges is considerably smaller than the relative amplitude of the temperature perturbation ($\delta n/n \approx 0.1 \delta T/T$). The perturbed particle flux is the quantity of interest as this also contributes to heat pulse transport. By considering a particle and heat flux of the form $\Gamma = -D \partial n/\partial r - Vn$, $Q = 3/2\Gamma T - n\chi\partial T/\partial r$, where D is the particle diffusion coefficient and V is the inwards particle drift velocity, it is then possible to include the enhanced heat flux due to a finite density perturbation. The equilibrium values of D and V are determined from the zero order particle flux as described above.

On TEXT the diffusion coefficient from density pulse measurements was found to be a factor of three larger than the value calculated from

equilibrium [7]. Allowance for an increased value of D and a relative perturbation value of $\delta n/n = 0.2 \delta T/T$ shows that the enhanced heat flux due to finite density perturbation leads to a reduction of 20% in the inferred value of χ_e . Work is in progress to consider the case in which the temperature and density perturbations are coupled by the off diagonal terms of the transport matrix. In this case particle and heat flux terms take the form $\Gamma = -D \partial n / \partial r - \alpha n / T \cdot \partial T / \partial r$, $Q = -\alpha T \partial n / \partial r - n \chi \partial T / \partial r + 3/2 \Gamma T$. Significant enhancement of the heat flux is found when $\alpha > 0.5 \chi_e$ is assumed.

5 TURBULENCE IN THE CORE

5.1 Diagnostics

Far infrared scattering and microwave reflectometry have been used to investigate the fluctuations in the plasma core which might cause the observed enhancement of particle and heat transport.

Wavenumber and frequency spectra of electron density fluctuations are measured with far infrared laser scattering along chords at different radii, including a horizontal chord through the plasma center and a vertical tangent at the outer edge. The system can be operated in homodyne and in heterodyne mode, where spectra for frequencies of both signs, corresponding to the different directions of propagation, are resolved. Reflectometry detects density fluctuations with spectral resolution at a selectable radius.

5.2 Results

Under ohmic conditions a number of parameter variations including electron density, electron temperature, toroidal magnetic field, and filling gas (H^+ , D^+ , He^{++}) were performed. Fig 1 shows a typical homodyne FIR k - ω spectrum from an ohmic hydrogen discharge at a chord radius of $25 \text{ cm} = 0.63a$.

The spectra observed fall into the wavenumber range predicted by numerical driftwave simulations. However, gyroradius scaling of k^{max} in the sense $k^{\text{max}} \propto \rho_S^{-1}$ is not found. In the dominant frequency range the rms value of the scattered power increases with the mean electron density, consistent with a fluctuation level determined by the mixing length criterion. In ohmic shots an asymmetry of the frequency spectra in the dominant wavenumber range is seen which increases with increasing line density. Since no effective spatial resolution across the minor radius exists at k^{max} this indicates an in-out asymmetry. At high k the fluctuations can be localized on the outer side, indicating propagation predominantly in the electron diamagnetic drift direction. In the SOC regime at high densities no separate feature emerges which would indicate an η_i -mode.

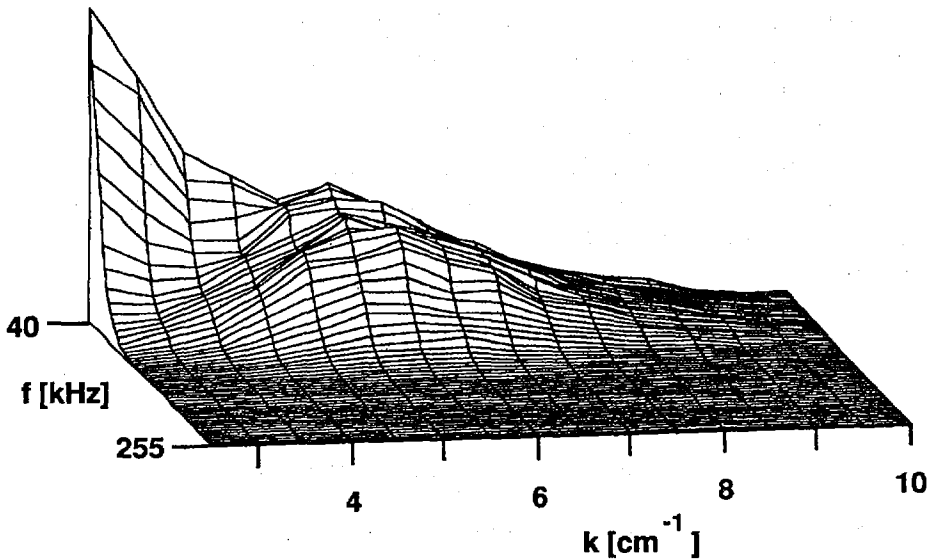


Fig. 1. Scattered signal power as function of wavenumber and frequency measured in an Ohmic discharge at a chord radius of 25 cm.

With neutral beam injection heating the k - ω spectra as well as the fluctuation levels change in a complex manner which depends sensitively on the heating scenario. In L-shots an increase of the fluctuation level together with a broadening of the frequency spectra and a shift which is possibly due to plasma rotation effects [8], [9] are measured. The k -spectra are shifted towards lower wavenumbers with no resolvable maximum.

The L-H transition manifests itself as a sudden change of the fluctuation spectra. The total scattered power decreases significantly to about ohmic level. The frequency spectra broaden and shift with respect to the L-phase. It must be pointed out, however, that in some cases an increase of the fluctuation level is detected by FIR and reflectometry during quiescent H-phases although the confinement remains unchanged. Fluctuations other than drift-type modes might be involved [10].

6 TURBULENCE IN THE EDGE REGION

6.1 Diagnostics

Langmuir probes were used to measure density and potential fluctuations in the edge region and in the divertor with good spatial and temporal resolution. Neglecting temperature fluctuations both parameters are derived from the ion saturation current and from the floating potential

respectively. Multiple probes and poloidal probe arrays with up to 17 pins yield simultaneously density and potential fluctuation measurements and details of their spatial evolution.

The observation of fluctuations in H_{α} emission from the edge with 16 photomultiplier channels allowed the temporal and spatial evolution of the edge density fluctuations to be studied in those cases where probes could not be used or an array with increased separation between channels was necessary.

6.2 Particle Transport

The radial particle flux due to the interaction of the fluctuating density with the fluctuating $E \times B$ drift was determined from :

$$\bar{\Gamma}_r = 1/2B_t \int_0^{\infty} \bar{k}_{pol}(\nu) |P_{n\Phi}(\nu)| \sin(\alpha_{n\Phi}(\nu)) d\nu$$

where $P_{n\Phi}$ is the cross-power spectrum of density and potential and k_{pol} is the average poloidal wave number at frequency ν . Within the limits of the accuracy of this method, the calculated particle flux is in agreement with the flux estimates from the confinement time [11]. We conclude that these fluctuations cause most if not all of the radial particle flux in the edge region.

Fig. 2 shows spectra of the different components contributing to the particle flux in comparison to the spectra of the density fluctuations at different radii. In the vicinity of the separatrix there is a strong low frequency component of fluctuations not contributing to the transport. This might indicate the transition to a region where a different type of fluctuation dominates the particle transport.

An evaluation based on the spatial Fourier transform indicates that fluctuations with wavenumbers around 2 cm^{-1} contribute most strongly to the particle flux.

6.3 Propagation and correlation lengths

Outside the separatrix the fluctuations propagate in the ion diamagnetic drift direction with a velocity of 500 - 1500 m/s corresponding to the local plasma velocity. Inside the separatrix the direction of propagation changes due to a strong shear of the poloidal plasma velocity.

Correlation lengths perpendicular to the magnetic field are of the order of one cm. Between a probe in the divertor and one in the midplane, a correlation above 80 % with zero time lag over a distance of 10 m was found. Within the limits of accuracy of measurement, both probe tips were located on the same field line. The edge turbulence is essentially 2-dimensional for frequencies up to at least 50 kHz.

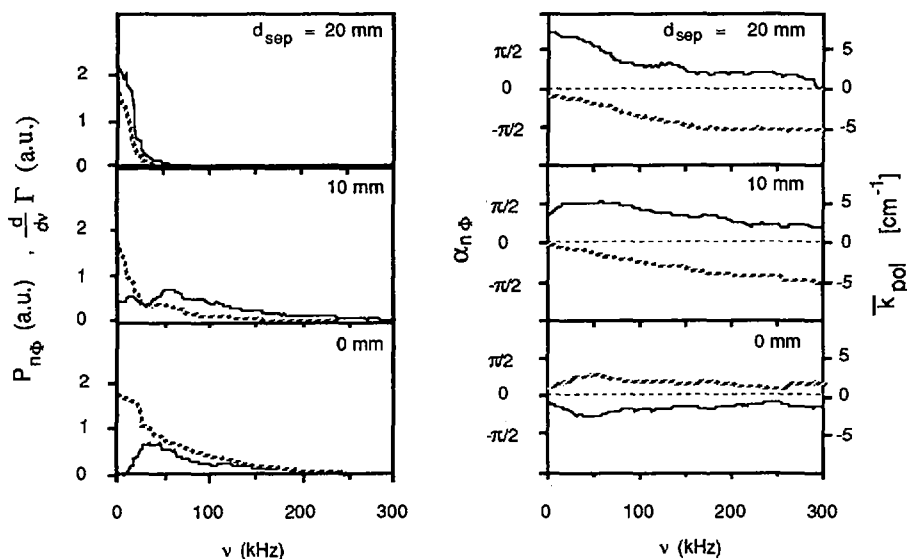


Fig. 2 Spectra of the different factors contributing to the particle flux. Left: Transport spectra (solid), cross-power spectrum of density and potential fluctuations. Right: Average phase angle between density and potential fluctuations (solid), mean poloidal wavenumber.

6.4 Asymmetry between low and high field side

In double null discharges no fluctuations are observed on the inboard edge of the torus. However, fluctuations with characteristics similar to the low field side are observed in single null discharges, that is when there is a connection along field lines to the outer edge. The turbulence seems to be driven at the outer edge, probably by the unfavourable curvature in this region.

7 CONCLUSIONS

The diffusion coefficients of the bulk plasma and impurities appear to vary with plasma parameters in exactly the same way as each other and in a similar way as the energy transport. Electrostatic turbulence involving convection with a scale length of the order of a banana width, which is typically 1 cm, might be able to produce this effect. Drift type fluctuations with k -spectra of this scale length are found in all discharges. There are some indications that they are connected with the changes in the particle and energy transport, as shown by the reduction of the fluctuation level at the L-H transition. Coupling between diffusion and inward particle drift and the

properties of the transient heat transport are experimental observations which impose boundary conditions on theoretical models. Experimental evidence for the relation between fluctuations and transport exists only at the edge outside the separatrix, where the fluctuations seem to be of a different nature. Their strong correlation in the region along the field lines suggests that their interaction with the target plates should play an important role.

REFERENCES

- [1] Gehre, O., Fussmann, G., Gentle, K.W. et al., Proc. 16th Eur. Conf. Venice, 1989, Europhysics Conference Abstracts **13B** Part I, 167.
- [2] Gentle, K.W., Gehre, O., Krieger, K., to be published in Nucl. Fusion.
- [3] Krieger, K., Fussmann, G., Determination of Impurity Transport Coefficients by Harmonic Analysis, accepted for publication by Nucl. Fusion.
- [4] Krieger, K., Fussmann, G., Proc. 17th Eur. Conf. Amsterdam, 1990, Europhysics Conference Abstracts **14B** Part III (1990) 1431.
- [5] Fussmann, G., Hofmann, J.V., Janeschitz, G. et al., J. Nucl. Mater. **162-164**, 14 (1989).
- [6] K. Riedel et al., Nucl. Fusion **28** (1988) 1503.
- [7] S. Kim et al., Phys. Rev. Lett. **60** (1988) 577.
- [8] Kallenbach, A., Mayer, H.-M., Fussmann, G. et al., Nuclear Fusion **30** (1990) 645
- [9] Hofmann, J.V., Field, A.R., Fussmann, G. et al., Proc. 17th Eur. Conf. Amsterdam, 1990, Europhysics Conference Abstracts **14B** Part IV (1990) 1556.
- [10] F.Wagner, IAEA-CN-53/A-4-2, this conference.
- [11] Rudyj, A. et al., Proc. 16th Eur. Conf. Venice, 1989, Europhysics Conference Abstracts **13B** Part I (1989) 27.

DISCUSSION

R.W. CONN: Since you take your measurement at the midplane boundary — and since we know that poloidal asymmetry in the flow is strong — how can you conclude, as you did, that fluctuation driven transport accounts for essentially all the particle transport? (You said it explains your global τ_p measurement.)

And a second question. Do you have any evidence of DC, steady convection at the edge in addition to the fluctuation driven flow? We see large flows of this kind in the continuous current tokamak (CCT). Results will be reported by Taylor later at the Conference.

H. NIEDERMEYER: We do not conclude that the fluctuations account for essentially all the particle transport, but for a major part of it — and possibly all. The relatively large error bars due to unknown asymmetries, the use of an approximate formula and the fact that temperature fluctuations are disregarded — all these things make a more precise statement unwise. We do not have any need for or any indication of another mechanism which would contribute significantly to the radial particle transport, but we cannot exclude the possibility that such a mechanism exists.

There is no evidence for stationary particle flows at the edge in addition to the fluctuation driven radial diffusion, poloidal and/or toroidal rotation of the plasma and the streaming-off into the divertor along field lines outside the separatrix. We believe that the symmetry of our magnetic field is adequate to keep magnetic islands inside the separatrix small enough so that radial particle flows along the field lines can be neglected. Magnetic probe measurements at the edge show that B-field fluctuations do not contribute significantly in good steady state discharge phases. Flows in bad discharges with high magnetic activity and during ELMs have not been investigated. As we do not yet know the findings from CCT, we cannot comment on them.

R.J. GOLDSTON: Burrell presented very interesting data which strongly suggest that the changes in outer region transport at the H-L transition are due to changes in the profiles in that region. This would imply that local edge fluctuations do not drive fluctuations and transport in the interior. Do you have information on the time scale for H-L changes in χ_e , χ_i or χ_ϕ at the edge of ASDEX?

H. NIEDERMEYER: Edge profiles and the energy flux across the separatrix change on a millisecond time-scale, indicating changes in edge transport coefficients on the same time-scale. The bulk transport reduces within 10 ms.